

3D QSAR studies on GSK-3 inhibition by aloisines

Min Zeng, Yongjun Jiang,* Bing Zhang, Kewen Zheng, Na Zhang and Qingsen Yu

*Key Laboratory for Molecular Design and Nutrition Engineering of Ningbo City, Ningbo Institute of Technology,
Zhejiang University, 315100 Ningbo, Zhejiang Province, PR China*

Received 11 August 2004; revised 21 October 2004; accepted 21 October 2004

Available online 11 November 2004

Abstract—GSK-3 is involved in various physiological processes and its inhibitors have been evaluated as promising drug candidates for a lot of unmet pathologies. In this paper, inhibition of GSK-3 by aloisines is investigated by 3D QSAR studies. Two alignment rules were applied to check the influence of spatial alignment of the compounds. Both the CoMFA and CoMSIA techniques were carried out and ASS procedure was applied for CoMFA to find a satisfactory model. The best QSAR model obtained is a CoMSIA model characterized with r^2 of 0.938 and q^2 of 0.673 including steric, electrostatic and hydrophobic fields, possessing good predicting ability. To get a better understanding of the relationship between chemical structure and biological activity, a complex structure of aloisine with GSK-3 was obtained by superimposing GSK-3 into the known cocrystal structure of aloisine-CDK2, and then factors that affect the inhibition activity were investigated further, combining the QSAR study with the complex structure, the results of which are in good accordance and complementary to each other.

© 2004 Elsevier Ltd. All rights reserved.

1. Introduction

Originally identified as a modulator of glycogen metabolism some 20 years ago, glycogen synthase kinase-3 (GSK-3) is now found to participate in a variety of cellular functions.^{1,2} As a well-established component of the Wnt signaling pathway and a ubiquitous serine/threonine protein kinase, GSK-3 is essential for embryonic development and plays important roles in protein synthesis, cell proliferation, cell differentiation, microtubule dynamics and cell motility, etc.; Higher functions, such as cognition and mood, may also be affected by GSK-3. Deregulation of GSK-3 could induce many metabolic and neurological disorders, including affective disorders, schizophrenia, stroke, head trauma, chronic inflammatory processes, cancer and Alzheimer's disease, etc.^{3,4} Nowadays, GSK-3 inhibitors have been evaluated as promising drug candidates.⁵

There are a lot of GSK-3 inhibitors, including indirubins, paullones, maleimides and lithium, etc.,^{6,7} and some new ones.^{8–12} In this paper, we report on study of aloisines (6-phenyl[5H]pyrrolo[2,3-b]pyrazines) as a

new family of GSK-3 inhibitor.¹³ 3D-QSAR (quantitative structure activity relationship) studies were carried out by both CoMFA (comparative molecular field analysis) and CoMSIA (comparative molecular similarity indices analysis) techniques to investigate factors that affect the inhibition activity. Two alignment rules were applied to check the influence of spatial alignment of the compounds and for CoMFA study all space searching (ASS) procedure was applied to find the satisfactory model. To aid the analysis, a complex structure of aloisine with GSK-3 was obtained by superimposing GSK-3 into the known cocrystal structure of aloisine-CDK2, and then factors that affect the inhibition activity were investigated further.

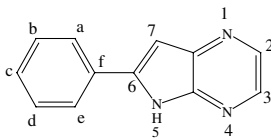
2. Methods

Discarding inactive compounds and compounds with unspecified activity, a data set composed of 35 aloisines was taken from the published paper,¹³ five of which were selected randomly to comprise a test set, leaving a training set of 30 compounds. Structures and experimental inhibition activities of all these aloisines are listed in Table 1.

Because in 3D QSAR study proper spatial alignment of the compounds is crucial in obtaining meaningful

Keywords: 3D-QSAR; GSK-3; Aloisines.

*Corresponding author. Tel.: +86 574 88229517; fax: +86 574 88229516; e-mail: yjjiang@nit.net.cn

Table 1. Structures and pIC₅₀ values of aloisines (compounds 01 to 30 are in training set)


No.	Substituents					Actual pIC ₅₀	Predicted pIC ₅₀	
	a	b	c	d	7		CoMSIA model	CoMFA model
01						5.64	5.73	5.39
02	OCH ₃					5.48	5.37	6.07
03	OH					5.19	5.37	5.78
04			OCH ₃			5.96	5.91	5.95
05			OH			5.92	5.78	5.73
06		OCH ₃		OCH ₃		4.22	4.23	5.96
07		OCH ₃	OCH ₃	OCH ₃		4.07	4.1	5.57
08			F			5.72	5.5	5.44
09			Br			5.22	5.26	5.83
10			CF ₃			5.14	5.05	6.17
11			CH ₃			5.59	5.57	5.26
12			CN			5.32	5.35	5.68
13			OCH ₃		CH ₃	6.34	6.19	5.06
14		OCH ₃	OCH ₃		CH ₃	5.70	5.76	5.19
15			OCH ₃		(CH ₂) ₃ Cl	5.60	5.61	6.03
16			OCH ₃		CH(CH ₃) ₂	6.30	6.37	6.27
17			OCH ₃		CH ₂ -CH=CH ₂	6.22	6.23	6.23
18			OCH ₃		(CH ₂) ₆ CH ₃	5.00	4.95	5.64
19			OCH ₃		CH ₂ C ₃ H ₅	5.96	6.03	5.85
20			OCH ₃		CH ₂ C ₆ H ₁₁	5.17	5.08	4.94
21			O-SO ₂ -N(CH ₃) ₂		CH ₃	6.30	6.35	5.97
22			Cl		CH ₃	5.77	5.83	6.37
23			Cl		CH(CH ₃) ₂	6.12	5.94	5.47
24			Cl		(CH ₂) ₃ CH ₃	5.23	5.24	5.32
25			Cl		CH ₂ C ₆ H ₅	5.17	5.47	3.98
26					CH ₂ C ₆ H ₅	6.00	5.82	5.57
27			OH		CH ₃	6.28	6.22	5.35
28			OH		(CH ₂) ₂ CH ₃	5.74	6.04	4.29
29			OH		CH ₂ C ₃ H ₅	5.52	5.79	5.62
30			OH		(CH ₂) ₃ CH ₃	6.19	5.94	6.11
31		OCH ₃				5.50	5.24	5.39
32			OCH ₃		(CH ₂) ₃ CH ₃	6.04	5.77	5.11
33			N(CH ₃) ₂			4.92	5.71	5.48
34			OCH ₃		(CH ₂) ₂ CH ₃	6.40	5.92	5.98
35			Cl		CH ₂ C ₆ H ₁₁	5.10	5.44	5.68

model,¹⁴ two alignment rules were applied in this study. In alignment 1 the template conformation (conformation 1 in Fig. 1) was extracted from the cocrystal structure of aloisine B (compound 23 in Table 1) with CDK2, a kinase that shares high homology with GSK-3. In alignment 2, the lowest energy conformation (conformation 2), which is found through a potential surface scan performed by Gaussian 98, is employed.

Then two sets of molecular were constructed and only the side chains were optimized, using AM1 method in BioMedCACH5.0. With Sybyl 6.8 molecular modeling software (Tripos Inc.), Gasteiger–Hückel charges were calculated, 3D structures were aligned based on template 1 and 2, respectively, generating two molecular aggregates. Since CoMFA model is highly sensitive to the space orientation of the molecular aggregate in the grid surrounding it, all-space searching (ASS) was employed to find the best CoMFA model, using Sybyl Pro-

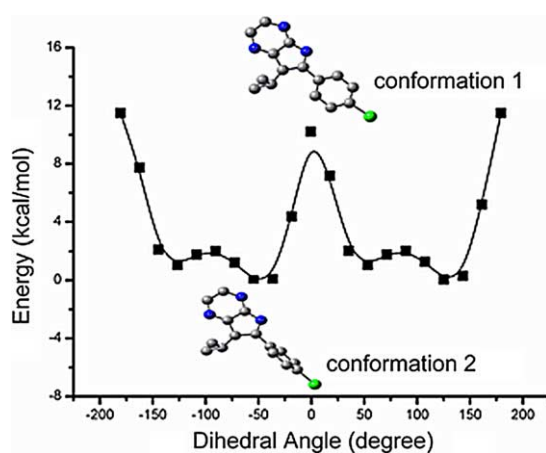


Figure 1. Two template conformations of aloisine B, shown in the plot got from potential surface scan of dihedral angle ef67 (see scheme in Table 1), performed by Gaussian 98 with b3lyp/6-31g* basis set.

gramming Language Script (SPL) written by Hou.¹⁵ Grid step was 2.0 Å for the entire generated database. The standard fields available in Sybyl 6.8 were calculated, using sp³ C-atom with +1 charge. The partial least square (PLS) method was applied to fit the 3D structural features with their biological activities and check for consistence and predicting ability of the models.

In order to aid the analysis, a complex structure of aloisine with GSK-3 was obtained. First, a structure of GSK-3 β , an isoform of GSK-3, was recovered from Brookhaven Protein Data Bank (entry code: 1UV5); Secondly, using the Biopolymer module in Sybyl 6.8, the structure of GSK-3 β was superimposed into the known cocrystal structure of aloisine-CDK2; Finally CDK2 was cut and the complex structure of aloisine with GSK-3 was obtained. Then combining the QSAR study with the complex structure, the inhibition of aloisine against GSK-3 was investigated further.

3. Results and discussion

For QSAR studies based on aggregate 1 and aggregate 2, the results of both the CoMFA and CoMSIA models are summarized in Table 2. It can be seen that after ASS CoMFA model was improved, for example, for CoMFA study based on aggregate 1 (CoMFA 1), r^2 changes from 0.432 to 0.584 after ASS and q^2 from 0.905 to 0.917. While for aggregate 2 (CoMFA 2), the best model obtained after ASS is still not satisfying, which has a q^2 of only 0.344, r^2 0.894 with five components, and the corresponding CoMSIA model (CoMSIA 2) is even worse. As seen from Figure 1, conformation 1 is much higher in energy than conformation 2. These lead to the conclusion that the bioactive conformation of the inhibitor is not supposed to be the lowest energy one.¹⁶ The reason for this may be that in complex with kinase, the inhibitor is confined by the kinase residues and interacts with them, so it cannot perform conformation change freely to lower its energy. In the following

discussion, we will focus only on the QSAR study based on aggregate 1.

Shown in Table 2, the best CoMSIA model based on aggregate 1 (highlighted in bold, with r^2 of 0.938, q^2 of 0.673), in which more than 1/3 (0.355) of the field contribution is from hydrophobic, is superior to the corresponding best CoMFA model, in which the hydrophobic field was not under consideration. These indicate that in the inhibition of GSK-3 by aloisine, hydrophobic interaction plays important roles, while the H-bond donor and acceptor fields do not possess such significance, manifested by the fact that all the other CoMSIA models that take into account these two fields do not generate good results. In the next, mainly the best CoMSIA model will be discussed.

The actual and predicted pIC₅₀ values of the best QSAR models are listed in Table 1 and the results of the best CoMSIA model is plotted in Figure 2, which shows that the predicted activities have good correlation with the actual ones and manifests the predicting ability of the model.

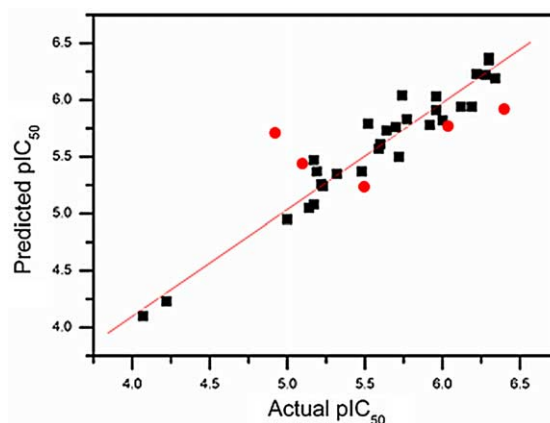


Figure 2. Actual pIC₅₀ versus predicted ones for the training set (squares) and the test set (circles) of CoMSIA 1 model.

Table 2. Summary of CoMFA and CoMSIA models for QSAR study

	q^2	r^2	SEE	F	No. Comp	Field contribution				
						S	E	H	D	A
<i>CoMFA 1</i>										
Before ASS	0.432	0.905	0.192	45.799	5	0.651	0.349			
After ASS	0.584	0.917	0.176	69.323	4	0.579	0.421			
<i>CoMFA 2</i>										
After ASS	0.344	0.894	0.200	48.765	5	0.696	0.304			
<i>COMSIA 1</i>										
S + E	0.567	0.900	0.201	34.504	6	0.416	0.584			
S + E + H	0.673	0.938	0.158	58.372	6	0.248	0.398	0.355		
S + E + H + D	0.664	0.954	0.142	55.05	8	0.233	0.328	0.335	0.103	
S + E + H + A	0.665	0.956	0.139	57.391	8	0.233	0.327	0.356		0.084
S + E + H + D + A	0.650	0.962	0.134	55.513	9	0.224	0.280	0.344	0.073	0.080
<i>CoMSIA 2</i>										
S + E + H	0.289	0.964	0.124	83.967	7	0.273	0.336	0.392		

CoMFA 1 and CoMSIA 1 are based on aggregate 1. CoMFA 2 and CoMSIA 2 are based on aggregate 2. S: steric field. E: electrostatic field. H: hydrophobic field. D: H-bond donor. A: H-bond acceptor. SEE: standard error of estimation.

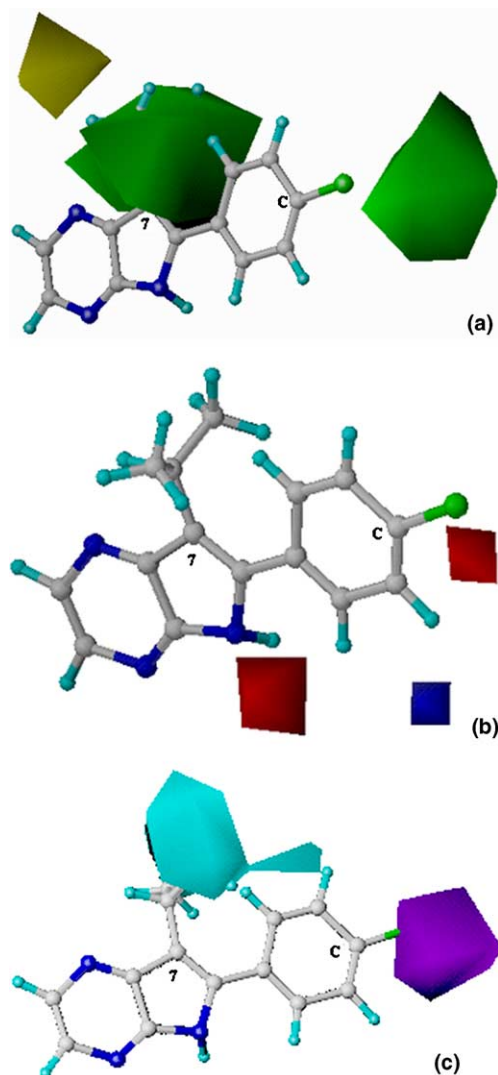


Figure 3. CoMSIA contour maps for steric (a), electrostatic (b), and hydrophobic (c) fields. Bulky groups in green region will increase activity, while in yellow regions decrease activity. Negative and positive charge rich groups are preferred in red and blue regions, respectively. Hydrophobic favored and disfavored regions are in cyan and purple, respectively.

The contour maps for the fields that are included in the best CoMSIA model are shown in Figure 3 with aloisine B as reference structure. As can be seen in Figure 3a, there is a sterically favored region (colored green) around the substituent on position 7, beyond which is a sterically unfavorable one (yellow), indicating that at position 7 only substituent large in a limited extent is helpful. Another sterically preferred area is near the substituent on position C. Negative and positive charge rich groups are helpful in red and blue region, respectively, as shown in Figure 3b. Plotted in Figure 3c, there is a hydrophobic preferred region (cyan) near position 7 and the purple region near position C means hydrophobic field there will decrease the inhibition activity.

Shown in Figure 4, the complex structure of aloisine B with GSK-3 β , aloisine B is located in the cleft between



Figure 4. Complex structure of aloisine B with GSK-3 β .

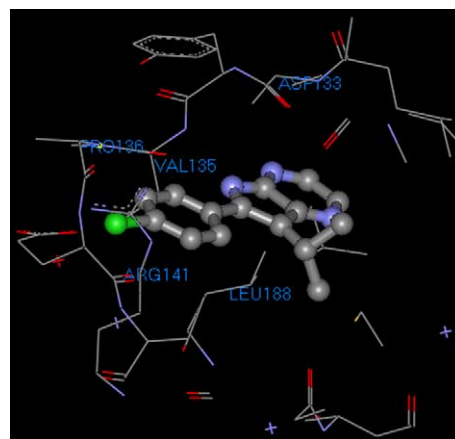


Figure 5. Residues that are within 5 Å around the inhibitor extracted from Figure 4.

two domains of GSK-3 β , which are beta-sheet and alpha-helix dominated, respectively. It reveals that substituent on position 7 is confined by the kinase residues near it, making it sterically restricted, so too large substituent on position 7 is detrimental for the inhibition activity. As for the substituent on position C, which pointing to the opening of the cleft, is not so sterically restricted and is exposed much to the ambient, so bulky substituent and hydrophilic field there should be helpful to the inhibition activity. To aid visualization, the residues within 5 Å around the inhibitor were extracted and shown in Figure 5. It shows that near the substituent on position 7, there is an apolar residue LEU188, which should interact with the substituent, so hydrophobic field would be preferred there. The positive charged residue ARG141 near position C makes negative-riched substituent favored there, and the O atom in residue VAL135, which pointing to the position d, makes positive-riched substituent there helpful.

4. Conclusion

In this paper, 3D QSAR studies were carried out to investigate the inhibition of aloisine against GSK-3.

Two alignment rules were applied, both the CoMFA and CoMSIA techniques were carried out and ASS procedure was applied for CoMFA to find satisfactory model. The template conformations of the two alignments applied in this study are conformation extracted from the cocrystal structure of aloisine B with CDK2 and the lowest energy one, respectively. The study shows that the bioactive conformation is not supposed to be the lowest in energy. The reason for this may be that in complex with kinase, the inhibitor cannot perform conformation change freely to lower its energy due to the confinement of kinase residues that interact with it. The best QSAR model obtained is characterized with r^2 of 0.938 and q^2 of 0.673 with six components for CoMSIA model. The model shows good predicting ability, enabling its application in rational design of new aloisines directed toward GSK-3 inhibition. It is demonstrated by the study that hydrophobic interaction plays important role in the inhibition. By superimposing the structure of GSK-3 into the known cocrystal structure of aloisine-CDK2, a complex structure of aloisine with GSK-3 was obtained. Factors that affect the inhibition activity were investigated further, combining the QSAR study with the complex structure, the results from which are in good accordance and complementary to each other. Still further study is being carried on to investigate the inhibition of aloisine against GSK in more detail.

Acknowledgements

The authors thank greatly Professor Laurent Meijer in Laboratory of Molecular and Cellular Neuroscience, the Rockefeller University, for the generous offering of the cocrystal structure of aloisine-CDK2 and we are grateful to Dr. Hou Tingjun of Peking University for the offering of ASS script. The author would like to thank the Doctor Foundation of Ningbo City, PR China for financial support (No. 2004A610018).

References and notes

1. Frame, S.; Cohen, P. *Biochem. J.* **2001**, *359*, 1–16.
2. Alonso, M.; Martinez, A. *Curr. Med. Chem.* **2004**, *11*, 755–763.
3. Wagman, A. S.; Johnson, K. W.; Bussiere, D. E. *Curr. Pharm. Des.* **2004**, *10*, 1105–1137.
4. Bhat, R. V.; Budd, S. L. *Neurosignals* **2002**, *11*, 251–261.
5. Van Wauwe, J.; Haefner, B. *Drug. News Perspect.* **2003**, *16*, 557–565.
6. Martinez, A.; Castro, A.; Dorronsoro, I.; Alonso, M. *Med. Res. Rev.* **2002**, *22*, 373–384.
7. Meijer, L.; Flajolet, M.; Greengard, P. *Trends. Pharmacol. Sci.* **2004**, *9*, 471–480.
8. Witherington, J.; Bordas, V.; Gaiba, A.; Naylor, A.; Rawlings, A. D.; Slingsby, B. P.; Smith, D. G.; Takle, A. K.; Ward, R. W. *Bioorg. Med. Chem. Lett.* **2003**, *13*, 3055–3057.
9. Witherington, J.; Bordas, V.; Gaiba, A.; Garton, N. S.; Naylor, A.; Rawlings, A. D.; Slingsby, B. P.; Smith, D. G.; Takle, A. K.; Ward, R. W. *Bioorg. Med. Chem. Lett.* **2003**, *13*, 3059–3062.
10. Gompel, M.; Leost, M.; De Kier Joffe, E. B.; Puricelli, L.; Franco, L. H.; Palermo, J.; Meijer, L. *Bioorg. Med. Chem. Lett.* **2004**, *14*, 1703–1707.
11. Peat, A. J.; Garrido, D.; Boucheron, J. A.; Schweiker, S. L.; Dickerson, S. H.; Wilson, J. R.; Wang, T. Y.; Thomson, S. A. *Bioorg. Med. Chem. Lett.* **2004**, *14*, 2127–2130.
12. Zhang, H. C.; Ye, H.; Conway, B. R.; Derian, C. K.; Addo, M. F.; Kuo, G. H.; Hecker, L. R.; Croll, D. R.; Li, J.; Westover, L.; Xu, J. Z.; Look, R.; Demarest, K. T.; Andrade-Gordon, P.; Damiano, B. P.; Maryanoff, B. E. *Bioorg. Med. Chem. Lett.* **2004**, *14*, 3245–3250.
13. Mettrey, Y.; Gompel, M.; Thomas, V.; Garnier, M.; Leost, M.; Ceballos-Picot, I.; Noble, M.; Endicott, J.; Vierfond, J. M.; Meijer, L. *J. Med. Chem.* **2003**, *46*, 222–236.
14. Kunick, C.; Lauenroth, K.; Wieking, K.; Xie, X.; Schultz, C.; Gussio, R.; Zaharevitz, D.; Leost, M.; Meijer, L.; Weber, A.; Jørgensen, F.; Lemcke, T. *J. Med. Chem.* **2004**, *47*, 22–36.
15. Hou, T. J.; Xu, X. J. *Chemometr. Intell. Lab. Syst.* **2001**, *56*, 123–132.
16. Huang, M.; Yang, D. Y.; Shang, Z.; Zou, J.; Yu, Q. *Bioorg. Med. Chem. Lett.* **2002**, *12*, 2271–2275.